Hindawi
Wireless Communications and Mobile Computing
Volume 2022, Article ID 8885240, 12 pages
https://doi.org/10.1155/2022/8885240

Research Article

Multi-Tag Selection in Cognitive Ambient Backscatter Communications for Next-Generation IoT Networks

Mi Ji Kim, Junsu Kim, and Su Min Kim

Department of Electronics Engineering, Korea Polytechnic University, Siheung 15073, Republic of Korea

Correspondence should be addressed to Su Min Kim; suminkim@kpu.ac.kr

Received 18 September 2020; Revised 14 August 2021; Accepted 27 December 2021; Published 31 January 2022

Academic Editor: Francois Chan

In this paper, we propose multi-tag selection schemes to improve achievable rate of a secondary ambient backscatter communication (ABC) system with multiple tags and a single power beacon in cognitive radio (CR) environments. Using the secondary power beacon, which plays a role as radio frequency (RF) source when there is no ambient RF source signals, with spectrum sensing capability, the secondary ABC system determines operation modes according to activity of the licensed primary system. When the primary system is active, a tag is randomly selected due to a lack of channel information, while when it is inactive, the best tag maximizing achievable rate is selected using the secondary power beacon. Moreover, we apply a successive interference cancellation (SIC) technique when the secondary power beacon is able to work. The performance of the proposed multi-tag selection schemes is mathematically analyzed in terms of bit error rate (BER) and achievable rate. Finally, the performance of the proposed schemes is evaluated through simulations in terms of BER and achievable rate. It is shown that our approach can significantly outperform a conventional ABC system in CR environments, especially under a low-active primary system regime.

1. Introduction

As Internet of things (IoT) era is coming, the number of wireless devices constructing IoT networks is explosively increasing. This causes a serious shortage in spectrum resource which is necessarily required for wireless connectivity. In order to solve this problem, many researchers have been conducting studies to improve spectral efficiency for large-scale wireless communications.

Recently, an ambient backscatter communication (ABC) system exploiting existing radio frequency (RF) signals such as TV, FM radio, and Wi-Fi was proposed [1]. It is a very promising IoT technology to solve the spectrum shortage problem as it does not require additional spectrum for communications [2]. Moreover, it enables wireless transmissions with very low power since ABC devices do not require an RF transceiver at transmitter side. Therefore, it is also promising to solve a battery problem of wireless IoT devices with combination of energy harvesting technologies [3–7].

In the ABC system, a tag, a passive transmitter that is not equipped with an RF transceiver, can modulate and transmit wireless signals by adjusting antenna impedance. That is, if it adjusts the impedance to absorb or reflect the ambient RF signals, a bit "0" or "1" is modulated, respectively. More specifically, in reflecting state, the tag maximally reflects the ambient signals so that the received power level is high at the receiver, where it is regarded as bit "1." On the contrary, in absorbing state, the tag absorbs the ambient signals as much as possible so that the received power level at the receiver is low, which leads to decide bit "0."

So far, there have been many studies on the ABC systems with various ambient RF signals such as FM radio [1], Wi-Fi [8–10], Bluetooth [11], ultra-wideband (UWB) [12], OFDM signals [13], and so on. For a variety of ambient signals, many researchers have been studying on signal modulation and coding [13, 14], semi-coherent [15] and non-coherent [16] detections, and performance analysis and approximation [17–19]. Thereafter, they are extended to multi-antenna systems [20, 21], cooperative

communications [22, 23], and multi-tag environments [24–30].

So far, there have been several studies on multi-tag ABC systems. In [24], a location-based tag-reader paring scheme was proposed to enhance bit error rate (BER) performance of the proposed ABC system. In [25], employing a multiple-input multiple-output (MIMO) reader, a least-squares-based channel estimation protocol and a low complexity algorithm were proposed in order to obtain the optimal transceiver designs to maximize backscattered throughput among multiple single-antenna tags. To exploit a multi-user diversity gain, several tag selection schemes have been proposed. In [19], a tag selection scheme was proposed to maximize BER at the receiver and its BER performance is mathematically analyzed. In [27, 28], tag selection schemes were proposed to improve secrecy outage and data rate in a wire-tap channel with a single eavesdropper. In [29, 30], artificial noise-aided tag scheduling schemes were proposed in order to maximize the secrecy rate. These studies mainly focus on performance improvements in the perspective of physical layer security in wire-tap channels.

On the other hand, cognitive radio (CR) communication, which allows unlicensed systems to share and utilize the spectrum bands of the licensed primary system when it is idle, is another promising technology to solve the spectrum shortage problem [31, 32]. There have been many studies on resource allocation and management in CR networks [33]. Among them, medium access control (MAC) protocols are designed and proposed for multi-user environments in both centralized and distributed manners [34–37]. In CR networks, sensing the primary system and reporting the sensing results to a secondary fusion node are important issues. Accordingly, there are several studies on the performance improvements in primary sensing [38] and reporting [39]. Recently, there are also a few studies on ABC systems under CR environments [40–42]. In these studies, the ABC system plays a role as an unlicensed secondary system under CR restrictions, where the secondary system is able to access the primary channel when it is only allowed by the primary system.

More specifically, in [40], an adaptive harvest-then-transmit protocol was proposed for an RF-powered cognitive radio network. In the proposed protocol, backscattering, harvesting, and transmitting modes are adaptively controlled to enhance transmission rate. In [41], error-floor-free detectors were proposed to tackle direct link interference using a multi-antenna receive beamforming technique in a cognitive ABC network which consists of a single tag and a single receiver as a secondary ABC system in a CR environment. Most recently, in [42], a novel spectrum sharing system was proposed to maximize data rate of secondary backscatter transmission subject to a minimum rate requirement of the primary system by jointly optimizing the time sharing and power allocation parameters. The previous work considers a new paradigm for IoT networks as cognitive backscatter communications where the secondary system exploits existing RF signals transmitted from the primary system. However, its performance can be limited by activity of the primary system since if there is no RF source signals, no backscatter information can be transmitted. Moreover, in previous work, only a single tag is considered although a basic feature of IoT networks is to require massive number of IoT devices in the network.

In this paper, we consider a secondary ABC system with multiple tags and a single power beacon, which can opportunistically access wireless channel of the licensed primary system under CR requirements. In this concept, according to the activity of the primary system, we propose adaptive multi-tag selection schemes to improve the performance of the secondary ABC system in terms of bit error rate (BER) and achievable rate. Therefore, the proposed schemes can significantly improve the performance of the secondary ABC system, especially under a low-active primary system regime. The contributions of this paper are summarized as follows:

(i) Employing a power beacon in the secondary CR system, a novel multi-tag selection scheme is proposed in order to improve the achievable rate of the secondary system in overlay CR environments.

(ii) The performance of the proposed multi-tag selection scheme is mathematically analyzed in terms of BER and achievable rate of the secondary system.

(iii) Through extensive simulations, the performance of the proposed multi-tag selection scheme is evaluated. It is shown that the proposed scheme can obtain additional spectral efficiency by improving average BER and activity of the secondary system.

The rest of this paper is organized as follows. In Section 2, the system model considered is illustrated. The proposed multi-tag selection schemes are presented in Section 3, and their performance analysis is provided in Section 4. In Section 5, numerical results for performance evaluation are shown. Finally, we conclude this paper in Section 6.

2. System Model

Figure 1 shows a secondary ABC system in a CR environment where primary and secondary systems coexist. The licensed primary system consists of a single transmitter generating RF signals and a single receiver. The secondary system consists of a single power beacon that transmits additional RF signals, K tags, and a single receiver. The activity of the primary system, which is a ratio of busy and idle states, is denoted by $\nu \in [0, 1]$. In the secondary ABC system, there are two operation modes according to the primary activity. If the primary system is active, the secondary ABC system modulates backscatter bits using the RF signals sent from the primary transmitter, while if the primary system is idle, it modulates backscatter bits using the RF signals generated by the secondary power beacon.

By employing a new power beacon as a part of the secondary ABC system, the secondary tags are still able to modulate and transmit their information to the secondary receiver by using the RF signals from the secondary power beacon, even if the primary system is idle. To this end, the secondary power beacon is capable to sense the primary channel and it generates

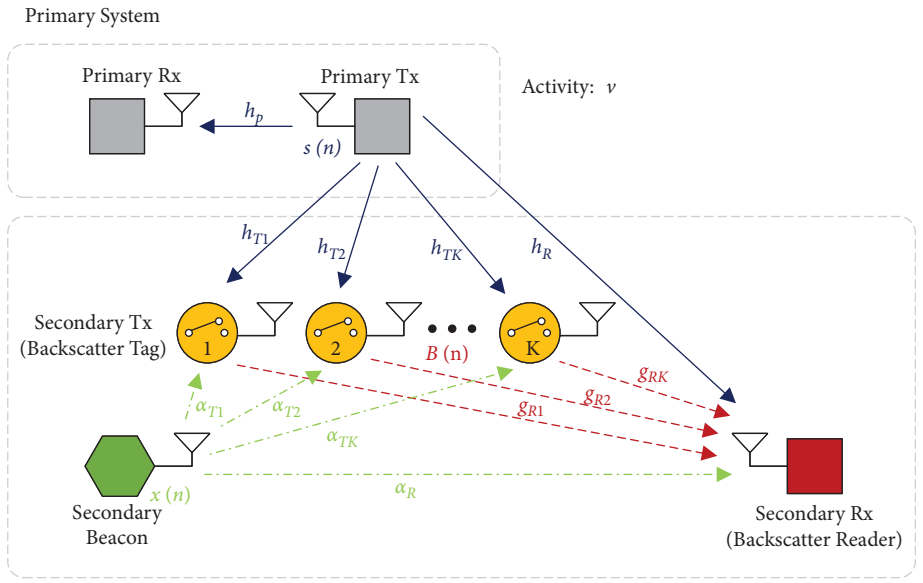

FIGURE 1: A cognitive ambient backscatter communication system with multiple tags and a single power beacon.

and transmits its own RF signals when the primary channel is decided as idle. Since the secondary power beacon is a part of the secondary system, the channel gains can be estimated at the secondary receiver using pilot signals, while it is impossible for the primary channel. Thus, we assume known channel information for the secondary power beacon and unknown channel information for the primary channel in this paper. It is worth noting that known channel information enables to apply for interference cancellation techniques.

In this system model, h_P, h_{T_i}, and h_R denote the channel gains between the primary transmitter and the primary receiver, the i-th tag, and the secondary receiver, respectively, α_{T_i} and α_R denote the channel gains between the secondary beacon and the i-th tag and the secondary receiver, respectively, and g_{R_i} denotes the channel gain between the i-th tag and the secondary receiver. We assume that all the channels suffer from i.i.d. block Rayleigh fading, i.e., $h_x \sim \mathcal{CN}(0, \sigma_{h_x}^2)$, $\alpha_x \sim \mathcal{CN}(0, \sigma_{\alpha_x}^2)$, $g_x \sim \mathcal{CN}(0, \sigma_{g_x}^2)$, $x \in \{R, T_i, R_i\}$, and $i \in \{1, 2, \ldots, K\}$, as in [26].

Figure 2 shows the frame structure of the secondary ABC system. In the training period, a preamble signal is transmitted to determine bit decision threshold values, Φ_0 and Φ_1, which imply the average received power values at the receiver when $B(n) = 0$ and $B(n) = 1$. That is, we consider a binary phase shift keying (BPSK) modulation for the secondary ABC system. A data frame consists of sensing, channel estimation, tag selection, and data transmission periods. In the sensing period, the secondary power beacon senses the primary channel using an energy detector (in this paper, we assume perfect sensing at the secondary power beacon; therefore, the performance of the proposed multi-tag selection scheme evaluated in this paper corresponds to the upper bound). Based on this, the primary activity is determined as either busy or idle. The channel gains h_x and α_x are estimated in the channel estimation period [43]. In the tag selection period, a single tag to transmit is scheduled. The channel estimation and tag selection are performed at the secondary receiver, and it is imformed to tags during the tag selection period. Finally, data transmission and detection are performed in the data transmission period. Note that since the secondary ABC system operates based on sensing at the secondary beacon, the secondary ABC system does not require synchronization with the primary system. However, the synchronization among the secondary beacon, multiple tags, and the secondary receiver is possible based on the frame structure in Figure 2.

3. Proposed Multi-Tag Selection Schemes

In this section, we propose multi-tag selection schemes to maximize achievable rate of the secondary ABC system considering the primary activity.

3.1. Tag Selection Schemes according to the Primary Activity

3.1.1. Status of the Primary System Is Busy. When the primary system is busy, the received signal at the secondary ABC receiver for the i-th tag and the n-th sample is given by

$$y(n) = h_R s(n) + \eta g_{R_i} h_{T_i} s(n) B(n) + \omega(n) = \begin{cases} h_R s(n) + \omega(n), & \text{if } B(n) = 0, \\ \left(h_R + \eta g_{R_i} h_{T_i}\right) s(n) + \omega(n), & \text{if } B(n) = 1, \end{cases} \quad (1)$$

where $s(n)$ denotes the primary RF signal, η denotes the antenna efficiency factor, $B(n)$ denotes the secondary backscatter bit, and $\omega(n)$ denotes the additive white Gaussian noise (AWGN) with zero mean and unit variance, i.e., $\omega(n) \sim \mathcal{CN}(0, \sigma_\omega^2)$. For this case, the channel estimation is impossible since the primary signal $s(n)$ is unknown at the secondary system. Thus, we randomly select a tag as follows:

$$i^* = \text{Uniform}(\{1, \ldots, K\}). \quad (2)$$

3.1.2. Status of the Primary System Is Idle. When the primary system is idle, we operate the secondary power beacon to

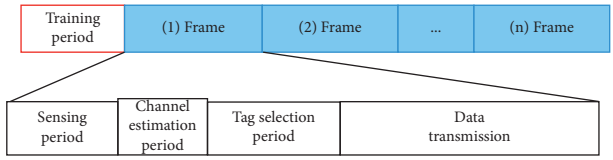

FIGURE 2: Frame structure of the secondary ABC system.

generate ambient RF signals artificially. Thus, the received signal at the secondary receiver for the i-th tag and the n-th sample is rewritten by

$$y(n) = \alpha_R x(n) + \eta g_{R_i} \alpha_{T_i} x(n) B(n) + \omega(n) = \begin{cases} \alpha_R x(n) + \omega(n), & \text{if } B(n) = 0, \\ \left(\alpha_R + \eta g_{R_i} \alpha_{T_i}\right) x(n) + \omega(n), & \text{if } B(n) = 1, \end{cases} \quad (3)$$

where $x(n)$ denotes the RF signal transmitted by the secondary power beacon.

Since the secondary power beacon is a part of the secondary system, the channel gains can be estimated for this case and we can employ a successive interference cancellation (SIC) technique at the secondary receiver. In the following, we present the proposed multi-tag selection schemes for both SIC-disabled and SIC-enabled cases.

(i) Tag selection without SIC: for this case, we apply a tag selection scheme maximizing BER proposed in [19]. Then, the selected tag is determined by

$$i^* = \arg\max_{i \in \{1,\ldots,K\}} \left| \left| \alpha_R + \eta \alpha_{T_i} g_{R_i} \right|^2 - \left| \alpha_R \right|^2 \right|. \quad (4)$$

(ii) Tag selection with SIC: for known $x(n)$, we can eliminate the interference term from the secondary power beacon based on the channel estimation [44]. This is possible since the power beacon is a part of the secondary system. Additionally, we assume the perfect channel estimation in order to investigate the performance upper bound. Then, the received signal for the i-th tag can be rewritten by

$$z(n) = y(n) - \widehat{\alpha}_R x(n) = \eta g_{R_i} \alpha_{T_i} x(n) B(n) + \omega(n) = \begin{cases} \omega(n), & \text{if } B(n) = 0, \\ \eta g_{R_i} \alpha_{T_i} x(n) + \omega(n), & \text{if } B(n) = 1, \end{cases} \quad (5)$$

where $\widehat{\alpha}_R$ is the estimated channel gain and with the perfect estimation, $\widehat{\alpha}_R = \alpha_R$. For this case, the best tag maximizing achievable rate is selected as follows:

$$i^* = \arg\max_{i \in \{1,\ldots,K\}} \left| \eta \alpha_{T_i} g_{R_i} \right|^2. \quad (6)$$

3.2. Detection Mechanism

3.2.1. Status of the Primary System Is Busy. When the primary system is busy, the decision thresholds, average received power levels during training period, for the i-th tag are determined by

$$\Phi_{0,i} = \frac{1}{N_0} \sum_{n=1}^{N_0} \left[\left| h_R \right|^2 P_s + \sigma_\omega^2 + 2 h_R s(n) \omega(n) \right], \quad (7)$$

$$\Phi_{1,i} = \frac{1}{N_0} \sum_{n=1}^{N_0} \left[\left| \mu_i \right|^2 P_s + \sigma_\omega^2 + 2 \mu_i s(n) \omega(n) \right], \quad (8)$$

where N_0 is the number of transmitted samples for a single backscatter bit during the training period, P_s is the average transmit power of the RF source signal $s(n)$, σ_ω^2 is the noise variance, and $\mu_i \triangleq h_R + \eta g_{R_i} h_{T_i}$. In the data transmission period, the selected i^*-th tag modulates and transmits a backscatter bit $B(n)$, and then the received signal at the secondary receiver is written by

$$y(n) = h_R s(n) + \eta g_{R_{i^*}} h_{T_{i^*}} s(n) B(n) + \omega(n). \quad (9)$$

The average received power at the secondary receiver during data transmission period can be calculated as

$$\Phi_B = \frac{1}{N_B} \sum_{n=1}^{N_B} |y(n)|^2 = \begin{cases} \left| h_R \right|^2 P_s + \sigma_\omega^2 + \Omega_{B_0}, & \text{if } B(n) = 0, \\ \left| \mu_{i^*} \right|^2 P_s + \sigma_\omega^2 + \Omega_{B_1}, & \text{if } B(n) = 1, \end{cases} \quad (10)$$

where

$$\Omega_{B_0} = \frac{2}{N_B} \sum_{n=1}^{N_B} \Re\left\{ h_R s(n) \omega(n)^H \right\}, \quad (11)$$

$$\Omega_{B_1} = \frac{2}{N_B} \sum_{n=1}^{N_B} \Re\left\{ \mu_{i^*} s(n) \omega(n)^H \right\}, \quad (12)$$

where N_B denotes the number of samples while transmitting a backscatter bit $B(n)$, $\Re(\cdot)$ denotes the real part of a complex number, and $(\cdot)^H$ is the conjugate and transpose operation. Note that the cross-correlation terms in (7), (8), (11), and (12) can be negligible for sufficiently large N_0 and N_B since $s(n)$ and $\omega(n)$ are statistically uncorrelated.

Finally, the backscattered bit $B(n)$ can be decoded at the secondary receiver with a comparison between the instantaneous average received power, Φ_B, and the threshold values, Φ_0 and Φ_1, as follows [17]:

$$\widehat{B}(n) = \begin{cases} 0, & \text{if } \left| \Phi_B - \Phi_{0,i^*} \right| \le \left| \Phi_B - \Phi_{1,i^*} \right|, \\ 1, & \text{if } \left| \Phi_B - \Phi_{0,i^*} \right| > \left| \Phi_B - \Phi_{1,i^*} \right|, \end{cases} = \begin{cases} 0, & \text{if } \Phi_B \le \xi, \\ 1, & \text{if } \Phi_B > \xi. \end{cases} \quad (13)$$

where $\xi = |h_R|^2 + |\mu_{i^*}|^2 / 2P_s$.

3.2.2. Status of the Primary System Is Idle. If the primary system is idle, the secondary power beacon is able to be active. Without SIC, the decision thresholds for the i-th tag are predetermined by

$$\Phi_{0,i} = \frac{1}{N_0}\sum_{n=1}^{N_0}\left[\left|\alpha_R\right|^2 P_x + \sigma_\omega^2 + 2\alpha_R x(n)\omega(n)\right],$$
$$\Phi_{1,i} = \frac{1}{N_0}\sum_{n=1}^{N_0}\left[\left|\varepsilon_i\right|^2 P_x + \sigma_\omega^2 + 2\varepsilon_i x(n)\omega(n)\right], \quad (14)$$

where P_x is the average transmit power of the secondary beacon signal $x(n)$, σ_ω^2 is the noise variance, and $\varepsilon_i \triangleq \alpha_R + \eta g_{R_i} h_{T_i}$. In the data transmission period, the received signal at the secondary receiver for the selected i^*-th tag is expressed as

$$y(n) = \alpha_R x(n) + \eta g_{R_{i^*}} \alpha_{T_{i^*}} x(n) B(n) + \omega(n). \quad (15)$$

Then, the average received power at the secondary receiver during data transmission period is calculated by

$$\Phi_B == \begin{cases} \left|\alpha_R\right|^2 P_x + \sigma_\omega^2 + \Omega'_{B0}, & \text{if } B(n) = 0, \\ \left|\varepsilon_{i^*}\right|^2 P_x + \sigma_\omega^2 + \Omega'_{B1}, & \text{if } B(n) = 1, \end{cases} \quad (16)$$

where

$$\Omega'_{B0} = \frac{2}{N_B}\sum_{n=1}^{N_B}\Re\left\{\alpha_R x(n)\omega(n)^H\right\},$$
$$\Omega'_{B1} = \frac{2}{N_B}\sum_{n=1}^{N_B}\Re\left\{\varepsilon_{i^*} x(n)\omega(n)^H\right\}. \quad (17)$$

Finally, the backscattered bit $B(n)$ can be decoded at the secondary receiver as follows:

$$\widehat{B}(n) = \begin{cases} 0, & \text{if } \Phi_B \le \xi', \\ 1, & \text{if } \Phi_B > \xi', \end{cases} \quad (18)$$

where $\xi' = |\alpha_R|^2 + |\varepsilon_{i^*}|^2/2P_x$.

With SIC, the decision thresholds for the i-th tag can be simplified as

$$\Phi_{0,i} = \frac{1}{N_0}\sum_{n=1}^{N_0}|\omega(n)|^2,$$
$$\Phi_{1,i} = \frac{1}{N_0}\sum_{n=1}^{N_0}\left|\eta g_{R_i}\alpha_{T_i} x(n) + \omega(n)\right|^2. \quad (19)$$

In the data transmission period, the received signal at the secondary receiver for the selected i^*-th tag is expressed as

$$y(n) = \eta g_{R_{i^*}} \alpha_{T_{i^*}} x(n) B(n) + \omega(n). \quad (20)$$

The average received power at the secondary receiver during data transmission period is rewritten by

$$\Phi_B = \begin{cases} \sigma_\omega^2, & \text{if } B(n) = 0, \\ \left|\rho_{i^*}\right|^2 P_x + \sigma_\omega^2 + \Omega''_{B1}, & \text{if } B(n) = 1, \end{cases} \quad (21)$$

where $\rho_i \triangleq \eta g_{R_i}\alpha_{T_i}$ and

$$\Omega''_{B_1} = \frac{2}{N_B}\sum_{n=1}^{N_B}\Re\left\{\rho_i x(n)\omega(n)^H\right\}. \quad (22)$$

Finally, the backscattered bit $B(n)$ can be decoded at the secondary receiver as follows:

$$\widehat{B}(n) = \begin{cases} 0, & \text{if } \Phi_B \le \xi'', \\ 1, & \text{if } \Phi_B > \xi'', \end{cases} \quad (23)$$

where $\xi'' = |\rho_{i^*}^2|/2P_x$.

4. Performance Analysis

In this section, we mathematically analyze the performance of the proposed multi-tag selection schemes in terms of BER and achievable rate. For analytical tractability, it is assumed that the channel between the selected tag and the secondary receiver, g_R, is line of sight and regarded as a constant as in [19]. This is reasonable since the distance between a tag and the secondary receiver is usually close in ABC networks.

4.1. Average BER. In this paper, BER is defined as a probability that the transmitted and estimated backscatter bits are not the same at the receiver. Thus, the BER for a single slot is expressed as

$$\begin{aligned} P_b &= \Pr\left(\widehat{B}(n) \ne B(n)\right) \\ &= \Pr\left(\widehat{B}(n) = 0 | B(n) = 1\right)\Pr\left(B(n) = 1\right) \\ &\quad + \Pr\left(\widehat{B}(n) = 1 | B(n) = 0\right)\Pr\left(B(n) = 0\right), \forall n. \end{aligned} \quad (24)$$

Note that bit "0" or "1" can be designed as equally probable in practice, and therefore $\Pr(B(n) = 0) = \Pr(B(n) = 1) = 0.5$ without loss of generality.

Hence, the average BER for a single frame which consists of multiple slots is given by

$$\begin{aligned} \overline{P}_b &= \mathbb{E}\left[P_b\right] = \mathbb{E}\left[\Pr\left(\widehat{B}(n) \ne B(n)\right)\right], \forall n, \\ &= \nu\overline{P}_b^{\text{busy}} + (1-\nu)\overline{P}_b^{\text{idle}}, \end{aligned} \quad (25)$$

where ν is the primary activity, $\overline{P}_b^{\text{busy}}$ is the average BER when the primary system is busy, and $\overline{P}_b^{\text{idle}}$ is the average BER when the primary system is idle.

In the following, we derive BER for a single slot and average BER when the primary system is either busy or idle. When it is idle, the secondary beacon is active in order to provide source RF signals. For this case, we also consider to employ the SIC technique in order to further improve the BER performance at the secondary receiver.

4.1.1. Random Tag Selection When the Primary System Is Busy. Let us recall $\mu_i \triangleq h_R + \eta g_{R_i} h_{T_i}$ and $\widetilde{\Phi}_B \triangleq \Phi_B - \sigma_\omega^2$. Similar to [19], for the selected i^*-th tag, if $|\mu_{i^*}|^2 > |h_R|^2$, conditional bit error probabilities of the energy detection are derived as

$$\begin{aligned}\Pr(\widehat{B}(n)=0|B(n)=1)&=\Pr\left(\widetilde{\Phi}_B<\xi|B(n)=1\right)\\&=\Pr\left(\Omega_{B_1}<-\frac{\left|\mu_{i^*}^2\right|-\left|h_R^2\right|}{2}P_s\right)\\&=Q\left(\frac{\left|\mu_{i^*}\right|^2-\left|h_R\right|^2}{\left|\mu_{i^*}\right|}\beta_s\right),\\\Pr(\widehat{B}(n)=1|B(n)=0)&=\Pr\left(\widetilde{\Phi}_B>\xi|B(n)=0\right)\\&=\Pr\left(\Omega_{B_0}>-\frac{\left|\mu_{i^*}\right|^2-\left|h_R\right|^2}{2}P_s\right)\\&=Q\left(\frac{\left|\mu_{i^*}\right|^2-\left|h_R\right|^2}{\left|h_R\right|}\beta_s\right),\end{aligned}\tag{26}$$

where $\xi=|h_R|^2+|\mu_{i^*}|^2/2P_s$ and $\beta_s=\sqrt{8\sigma_\omega^2/N_BP_s}$.

If $|\mu_{i^*}|^2<|h_R|^2$, they are rewritten, respectively, by

$$\begin{aligned}\Pr(\widehat{B}(n)=0|B(n)=1)&=Q\left(-\frac{\left|\mu_{i^*}\right|^2-\left|h_R\right|^2}{\left|\mu_{i^*}\right|}\beta_s\right),\\\Pr(\widehat{B}(n)=1|B(n)=0)&=Q\left(-\frac{\left|\mu_{i^*}\right|^2-\left|h_R\right|^2}{\left|h_R\right|}\beta_s\right).\end{aligned}\tag{27}$$

Substituting (32)–(35) into (24) and assuming $\Pr(B(n)=1)=\Pr(B(n)=0)=0.5$, BER for a single slot can be derived as

$$P_b^{\text{busy}}=\frac{1}{2}\left[Q\left(\frac{\left|\left|\mu_{i^*}\right|^2-\left|h_R\right|^2\right|}{\left|\mu_{i^*}\right|}\beta_s\right)+Q\left(\frac{\left|\left|\mu_{i^*}\right|^2-\left|h_R\right|^2\right|}{\left|h_R\right|}\beta_s\right)\right].\tag{28}$$

Thus, average BER over all slots is obtained as

$$\begin{aligned}\overline{P}_b^{\text{busy}}&=\mathbb{E}\left[P_b^{\text{busy}}\right]\\&=\frac{1}{2}\left[\int_0^\infty Q(\beta_s m)f_{M_1}(m)\,\mathrm{d}m+\int_0^\infty Q(\beta_s n)f_{N_1}(n)\,\mathrm{d}n\right],\end{aligned}\tag{29}$$

where $M_1=||\mu_{i^*}|^2-|h_R|^2|/|\mu_{i^*}|$ and $N_1=||\mu_{i^*}|^2-|h_R|^2|/|h_R|$.

Unfortunately, since the channel gains are not known exactly, it is hard to find the exact PDFs of M_1 and N_1. However, the average BER can be approximated as [19]

$$\overline{P}_b^{\text{busy}}\approx\frac{1}{2}\int_0^\infty\left[Q(\beta_1 z)+Q(\beta_2 z)\right]f_{|Y_{i^*}|}(z)\,\mathrm{d}z,\tag{30}$$

where $\beta_{s,1}=\beta_s/C_1\sigma_{\mu_{i^*}}$, $\beta_{s,2}=\beta/C_2\sigma_{h_R}$, $\beta_s=\sqrt{8\sigma_\omega^2/N_BP_s}$, and C_1 and C_2 are constants that are determined by the number of tags and channel variances. Here, since we select a tag randomly, assuming i.i.d. block Rayleigh fading, the PDF of $|Y_{i^*}|$ is obtained by

$$f_{|Y_{i^*}|}(y)=\frac{1}{\sigma_{\mu_{i^*}}^2+\sigma_{h_R}^2}\left(e^{-1/\sigma_{\mu_{i^*}}^2y}+e^{-1/\sigma_{h_R}^2y}\right),\quad y>0,\tag{31}$$

where $Y_{i^*}\triangleq|\mu_{i^*}|^2-|h_R|^2$.

4.1.2. Tag Selection without SIC When the Primary System Is Idle. Hereafter, we derive average BER without employing the SIC technique when the primary system is inactive.

Let us recall $\varepsilon_i\triangleq\alpha_R+\eta g_{R_i}\alpha_{T_i}$ and $\widetilde{\Phi}_B\triangleq\Phi_B-\sigma_\omega^2$. Similar to the BER derivation when the primary system is busy, for the selected i^*-th tag, if $|\varepsilon_{i^*}|^2>|\alpha_R|^2$, conditional bit error probabilities of the energy detection are derived as

$$\Pr(\widehat{B}(n)=0|B(n)=1)=Q\left(\frac{\left|\varepsilon_{i^*}\right|^2-\left|\alpha_R\right|^2}{\left|\varepsilon_{i^*}\right|}\beta_x\right),\tag{32}$$

$$\Pr(\widehat{B}(n)=1|B(n)=0)=Q\left(\frac{\left|\varepsilon_{i^*}\right|^2-\left|\alpha_R\right|^2}{\left|\alpha_R\right|}\beta_x\right),\tag{33}$$

where $\xi'=|\alpha_R|^2+|\varepsilon_{i^*}|^2/2P_x$ and $\beta_x=\sqrt{8\sigma_\omega^2/N_BP_x}$.

If $|\varepsilon_{i^*}|^2<|\alpha_R|^2$, they are rewritten, respectively, by

$$\Pr(\widehat{B}(n)=0|B(n)=1)=Q\left(-\frac{\left|\varepsilon_{i^*}\right|^2-\left|\alpha_R\right|^2}{\left|\varepsilon_{i^*}\right|}\beta_x\right),\tag{34}$$

$$\Pr(\widehat{B}(n)=1|B(n)=0)=Q\left(-\frac{\left|\varepsilon_{i^*}\right|^2-\left|\alpha_R\right|^2}{\left|\alpha_R\right|}\beta_x\right).\tag{35}$$

Substituting (32)–(35) into (24) and assuming $\Pr(B(n)=1)=\Pr(B(n)=0)=0.5$, BER for a single slot can be derived as

$$P_b^{\text{idle}}=\frac{1}{2}\left[Q\left(\frac{\left|\left|\varepsilon_{i^*}\right|^2-\left|\alpha_R\right|^2\right|}{\left|\varepsilon_{i^*}\right|}\beta_x\right)+Q\left(\frac{\left|\left|\varepsilon_{i^*}\right|^2-\left|\alpha_R\right|^2\right|}{\left|\alpha_R\right|}\beta_x\right)\right].\tag{36}$$

Thus, average BER over all slots is obtained as

$$\overline{P}_b^{\text{idle}}=\mathbb{E}\left[P_b^{\text{idle}}\right]=\frac{1}{2}\left[\int_0^\infty Q(\beta_x m)f_{M_2}(m)\,\mathrm{d}m+\int_0^\infty Q(\beta_x n)f_{N_2}(n)\,\mathrm{d}n\right],\tag{37}$$

where $M_2 = ||\varepsilon_{i^*}|^2 - |\alpha_R|^2|/|\varepsilon_{i^*}|$ and $N_2 = ||\varepsilon_{i^*}|^2 - |\alpha_R|^2|/|\alpha_R|$.

Since it is hard to find the exact PDFs of M_2 and N_2, using Theorem 1 in [19], the average BER can be approximated as

$$\overline{P}_b^{\text{idle}} \approx \frac{1}{2}\int_0^{\infty}\left[Q\left(\beta_{x,1}z\right) + Q\left(\beta_{x,2}z\right)\right] f_{|Z_{i^*}|}(z)\,\mathrm{d}z, \tag{38}$$

where $Z_{i^*} \triangleq |\varepsilon_{i^*}|^2 - |\alpha_R|^2$, $\beta_{x,1} = \beta_x/D_1\sigma_{\varepsilon_{i^*}}$, $\beta_{x,2} = \beta_x/D_2\sigma_{\alpha_R}$, $\beta_x = \sqrt{8\sigma_\omega^2/N_B P_s}$, and D_1 and D_2 are constants that are determined by the number of tags and channel variances. For this case, since the best tag i^* is selected according to (6), the PDF of $|Z_{i^*}|$ is obtained by [19]

$$f_{|Z_{i^*}|}(z) = \frac{K}{\sigma_{\varepsilon_{i^*}}^2 + \sigma_{\alpha_R}^2}\left(e^{-1/\sigma_{\varepsilon_{i^*}}^2 z} + e^{-1/\sigma_R^2 z}\right)$$

$$\cdot\left(1 - \frac{\sigma_{\varepsilon_{i^*}}^2}{\sigma_{\varepsilon_{i^*}}^2 + \sigma_{\alpha_R}^2}e^{-1/\sigma_{\varepsilon_{i^*}}^2 z} - \frac{\sigma_{\alpha_R}^2}{\sigma_{\varepsilon_{i^*}}^2 + \sigma_{\alpha_R}^2}e^{-1/\sigma_{\alpha_R}^2 z}\right)^{K-1}, \quad z > 0, \tag{39}$$

where K denotes the number of tags.

4.1.3. Tag Selection with SIC When the Primary System Is Idle. When SIC is employed, since the interference from the RF source is eliminated, the analysis can be simplified. Similar to the case without SIC, we first define $\rho_i \triangleq \eta g_{R_i}\alpha_{T_i}$ and $\widetilde{\Phi}_B \triangleq \Phi_B - \sigma_\omega^2$. Since $|\rho_i|^2 > 0$, the BER for a single slot can be obtained as

$$\begin{aligned}\Pr\left(\widehat{B}(n) = 0 | B(n) = 1\right) &= \Pr\left(\widetilde{\Phi}_B < \xi'' | B(n) = 1\right)\\ &= \Pr\left(\Omega_{B_1}'' < -\frac{|\rho_{i^*}|^2}{2}P_x\right)\\ &= Q\left(|\rho_{i^*}|\beta\right),\end{aligned} \tag{40}$$

$$\begin{aligned}\Pr\left(\widehat{B}(n) = 1 | B(n) = 0\right) &= \Pr\left(\widetilde{\Phi}_B > \xi'' | B(n) = 0\right)\\ &= \Pr\left(\Omega_{B_0}'' > -\frac{|\rho_{i^*}|^2}{2}P_x\right) = 0,\end{aligned} \tag{41}$$

where $\beta_x = \sqrt{8\sigma_\omega^2/N_B P_x}$.

Substituting (40) and (41) into (24) and assuming $\Pr(B(n) = 1) = \Pr(B(n) = 0) = 0.5$, BER for a single slot can be simplified as

$$P_b^{\text{idle}} = \frac{1}{2}Q\left(|\rho_{i^*}|\beta_x\right). \tag{42}$$

Finally, the average BER for all slots is obtained as

$$\overline{P}_b^{\text{idle}} = \mathbb{E}\left[P_b^{\text{idle}}\right] = \frac{1}{2}\int_0^{\infty} Q\left(|\rho_{i^*}|\beta_x\right) f_{|\rho_{i^*}|}(z)\,\mathrm{d}z, \tag{43}$$

where

$$f_{|\rho_{i^*}|}(z) = \frac{1}{\sigma_{\rho_{i^*}}^2}\left(e^{-1/\sigma_{\rho_{i^*}}^2 z}\right)\left(1 - e^{-1/\sigma_{\rho_{i^*}}^2 z}\right)^{K-1}, \quad z > 0, \tag{44}$$

and $\sigma_{\rho_{i^*}}^2 = \eta^2\sigma_{\alpha_{T_{i^*}}}^2\sigma_{g_{R_{i^*}}}^2$ and K is the number of tags.

4.2. Average Achievable Rate. Based on the obtained BERs, average achievable rate of the secondary ABC system is expressed as

$$\overline{R}_B^x = R_s\frac{N_B\left(1 - \overline{P}_b^x\right)}{N_{\text{tot}}}, \; x \in \{\text{busy, idle}\}, \tag{45}$$

where R_s is the source data rate of the primary signal $s(n)$, N_B is the number of backscattered bits, and N_{tot} is the total number of transmitted bits. $\overline{P}_b^x$ are obtained in (30), (38), and (43).

Finally, the average achievable rate of the proposed secondary ABC systems is expressed as

$$\overline{R}_B = \nu\overline{R}_B^{\text{busy}} + (1 - \nu)\overline{R}_B^{\text{idle}}, \tag{46}$$

where ν is the primary activity.

5. Numerical Results

In this section, we evaluate the performance of the proposed multi-tag selection schemes in terms of BER and average achievable rate of the secondary ABC system through simulations. Throughout the simulations, we set unit i.i.d. channel gains for all the links, i.e., $\sigma_{h_x}^2 = \sigma_{\alpha_x}^2 = \sigma_{R_x}^2 = 1$, $i \in \{1, 2, \ldots, K\}$.

Figures 3 and 4 show the BER and the average achievable rate of the secondary ABC system for varying primary activity when the number of tags $K = 8$ and SNR = 15 dB. When the primary system is always busy, i.e., $\nu = 1$, all the schemes obtain the same BER and achievable rate. However, as shown in Figure 4, as the primary activity decreases, the achievable rate of the conventional scheme significantly degrades due to absence of ambient RF source signals, while those of the proposed multi-tag selection schemes are kept or even improved with SIC. Especially, for the proposed multi-tag selection scheme with SIC, the BER is further improved as the primary activity is decreased, while the BERs of both the proposed multi-tag selection scheme without SIC and the conventional scheme are almost maintained as the primary activity is getting low as shown in Figure 3. As a result, the proposed cognitive ABC system with multi-tag selection schemes can provide significantly improved achievable rate even under limited spectrum resource.

Figures 5 and 6 show the BER and the average achievable rate of the secondary ABC system for varying SNR when $\nu = 0.1$. In Figure 5, it is shown that the BERs of the proposed multi-tag selection schemes with and without SIC are reduced, as the number of tags increases due to a selection diversity gain, while that of the conventional scheme is invariant. In addition, the proposed multi-tag selection scheme with SIC significantly outperforms that without SIC in high SNR regime. On the other hand, as shown in Figure 6, the achievable rate of the conventional scheme is very small with low primary activity, regardless of SNR and the number of tags. On the contrary, the proposed multi-tag selection schemes provide sufficient achievable rates in the whole range of SNRs. Furthermore, they can obtain a selection diversity gain, and thus their achievable rates

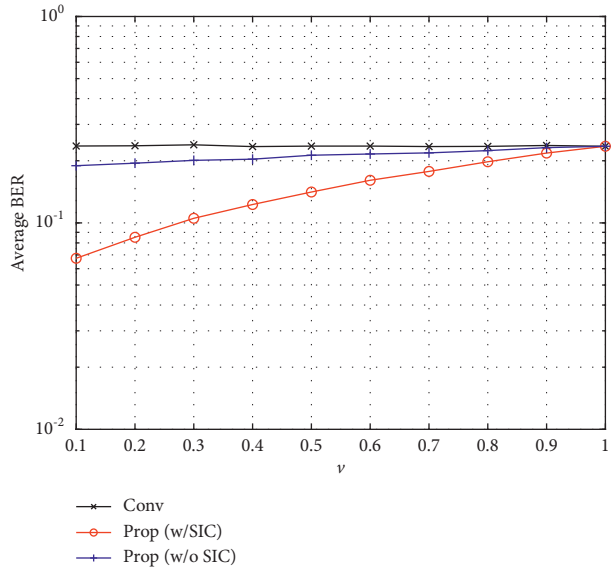

Figure 3: Average BER of the secondary ABC system for varying primary activity ($K = 8$ and SNR = 15 dB).

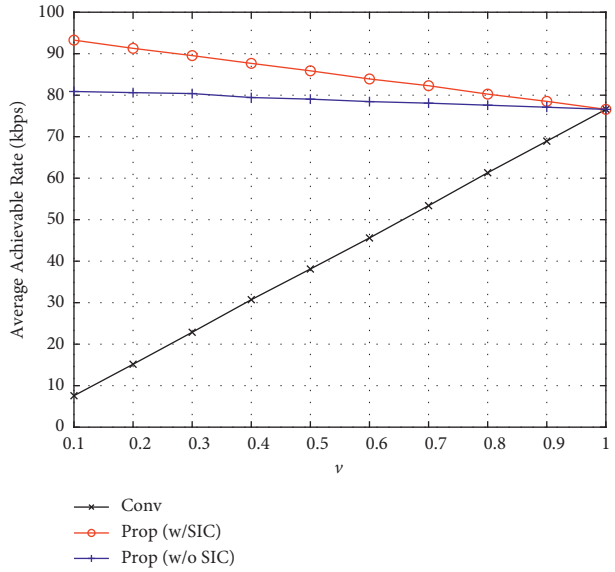

Figure 4: Average achievable rate of the secondary ABC system for varying primary activity ($K = 8$ and SNR = 15 dB).

increase as the number of tags increases, regardless of the primary activity. Additionally, the proposed multi-tag selection scheme with SIC always outperforms that without SIC thanks to the improved BER performance.

Figures 7 and 8 show the BER and the average achievable rate of the secondary ABC system for varying the number of tags when $\nu = 0.3$ and SNR = 15 dB. In the figures, it is shown that the BERs and the achievable rates of the proposed multi-tag selection schemes are almost converged to the best performance when the number of tags is more than five. This implies that only a small number of tags are enough to achieve sufficiently good performance. On the contrary, the BER of the conventional scheme is not affected by the number of tags and its average rate is significantly low, compared to those of the proposed multi-tag selection schemes with and without SIC. This is because in the conventional scheme, the secondary ABC system cannot operate during idle period of the primary system due to absence of the ambient RF source signal. However, in the proposed multi-tag selection-based cognitive ABC system, a power beacon with spectrum sensing capability for the primary channel can provide the ambient RF source signal to the tags, although the primary system is silent.

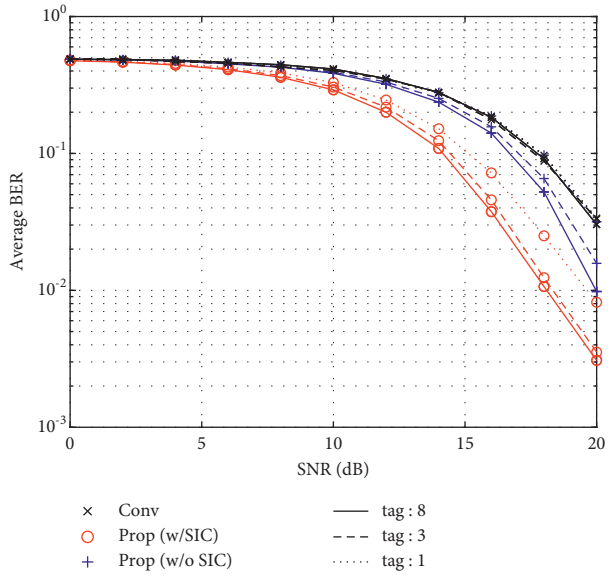

Figure 5: Average BER of the secondary ABC system for varying SNR ($\nu = 0.1$).

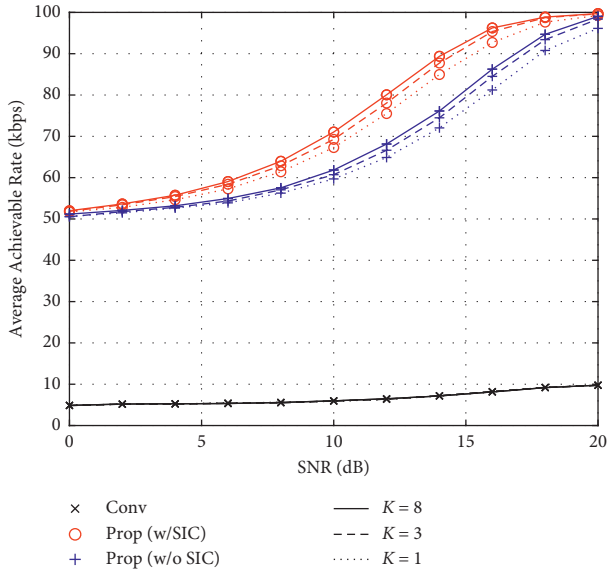

Figure 6: Average achievable rate of the secondary ABC system for varying SNR ($\nu = 0.1$).

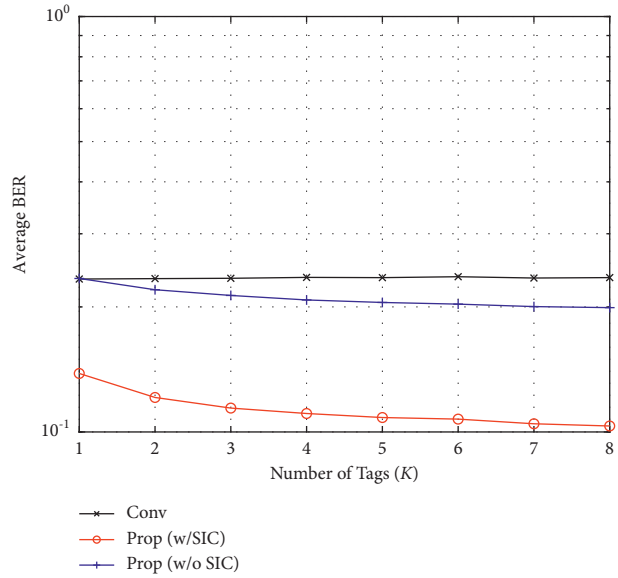

Figure 7: Average BER of the secondary ABC system for varying number of tags ($\nu = 0.3$ and SNR = 15 dB).

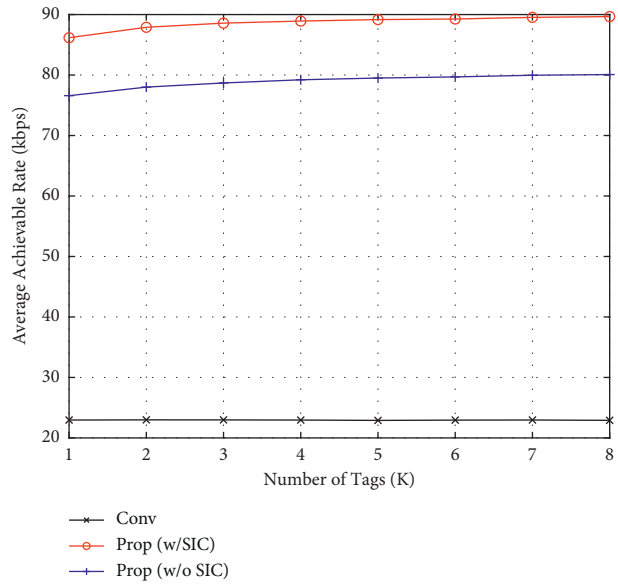

Figure 8: Average achievable rate of the secondary ABC system for varying number of tags ($\nu = 0.3$ and SNR = 15 dB).

6. Conclusion

In this paper, we proposed multi-tag selection schemes to improve the achievable rate of a secondary ABC system under CR environments. The performance of the proposed schemes was mathematically derived and evaluated through simulations. It is shown that the proposed multi-tag selection scheme without SIC can significantly improve the performance, compared to the conventional scheme, thanks to additional secondary power beacon and selection diversity gain. By applying SIC, it is further enhanced with reduced BER performance obtained from an interference cancellation technique. Further work will allow the power beacon to control the transmit power level and optimize it under given power constraint in order to design an energy-efficient secondary ABC system. In addition, incorporation of energy harvesting or conservation strategies for the secondary power beacon can be also considered. Furthermore, the impact of imperfect sensing at the secondary power beacon and machine learning-based detecting approaches for imperfect channel information conditions can be another research topic.

Data Availability

The data used to support the finding of this study are included within the article.

Conflicts of Interest

The authors declare that they have no conflicts of interest.

Acknowledgments

This study was supported in part by the MSIT, Korea, under the ITRC Support Program (IITP-2021-2018-0-01 426) supervised by the IITP and in part by the National Research Foundation of Korea (NRF) grant funded by the Korean Government (MSIT) (no. 2019R1F1A1059125).

References

[1] V. Liu, A. N. Parks, V. Talla, S. Gollakota, D. Wetherall, and J. R. Smith, "Ambient backscatter: wireless communication out of thin air," in *Proceedings of the ACM Special Interest Group on Data Communication (SIGCOMM)*, Hong Kong, China, August 2013.

[2] N. Van Huynh, D. T. Hoang, X. Lu, D. Niyato, P. Wang, and D. I. Kim, "Ambient backscatter communications: a contemporary survey," *IEEE Communications Surveys & Tutorials*, vol. 20, no. 4, pp. 2889–2922, 2018.

[3] X. Lu, P. Wang, D. Niyato, D. I. Kim, and Z. Han, "Wireless networks with RF energy harvesting: a contemporary survey," *IEEE Communications Surveys & Tutorials*, vol. 17, no. 2, pp. 757–789, 2015.

[4] P. Kamalinejad, C. Mahapatra, Z. Sheng, S. Mirabbasi, V. C. M. Leung, and Y. L. Guan, "Wireless energy harvesting for the internet of things," *IEEE Communications Magazine*, vol. 53, no. 6, pp. 102–108, 2015.

[5] I. Bang, S. M. Kim, and D. K. Sung, "Adaptive multiuser scheduling for simultaneous wireless information and power transfer in a multicell environment," *IEEE Transactions on Wireless Communications*, vol. 16, no. 11, pp. 7460–7474, 2017.

[6] K. Han and K. Huang, "Wirelessly powered backscatter communication networks: modeling, coverage, and capacity," *IEEE Transactions on Wireless Communications*, vol. 16, no. 4, pp. 2548–2561, 2017.

[7] A. N. Parks, A. Liu, S. Gollakota, and J. R. Smith, "Turbocharging ambient backscatter communication," *ACM Special Interest Group on Data Communication (SIGCOMM)*, vol. 444, 2014.

[8] B. Kellogg, A. Parks, S. Gollakota, J. R. Smith, and D. Wetherall, "Wi-Fi backscatter: internet connectivity for RF-powered devices," *ACM Special Interest Group on Data Communication (SIGCOMM)*, vol. 44, no. 4, 2014.

[9] D. Bharadia, K. R. Joshi, M. Kotaru, and S. Katti, "BackFi: high throughput WiFi backscatter," *ACM Special Interest Group on Data Communication (SIGCOMM)*, vol. 45, no. 4, 2015.

[10] B. Kellogg, V. Talla, S. Gollakota, and J. R. Smith, "Passive wi-fi: bringing low power to wi-fi transmissions," *USENIX Symposium on Networked Systems Design and Implementation (NSDI)*, vol. 20, no. 3, 2016.

[11] V. L. V. Talla, B. Kellogg, S. Gollakota, and J. R. Smith, "Inter-technology backscatter: towards Internet connectivity for implanted devices," in *Proceedings of the ACM Special Interest Group on Data Communication (SIGCOMM)*, Hong Kong, China, August 2016.

[12] C. Yang, J. Gummeson, and A. Sample, "Riding the airways: ultra-wideband Ambient backscatter via commercial broadcast systems," in *Proceedings of the IEEE International Conference on Computer Communications (INFOCOM)*, Atlanta, GA, USA, May 2017.

[13] G. Yang, Y.-C. Liang, R. Zhang, and Y. Pei, "Modulation in the air: backscatter communication over ambient OFDM carrier," *IEEE Transactions on Communications*, vol. 66, no. 3, pp. 1219–1233, 2018.

[14] Y. Liu, G. Wang, Z. Dou, and Z. Zhong, "Coding and detection schemes for ambient backscatter communication systems," *IEEE Access*, vol. 5, pp. 4947–4953, 2017.

[15] J. Qian, F. Gao, G. Wang, S. Jin, and H. Zhu, "Semi-coherent detection and performance analysis for ambient backscatter system," *IEEE Transactions on Communications*, vol. 65, no. 12, pp. 5266–5279, 2017.

[16] J. Qian, F. Gao, G. Wang, S. Jin, and H. Zhu, "Noncoherent detections for ambient backscatter system," *IEEE Transactions on Wireless Communications*, vol. 16, no. 3, pp. 1412–1422, 2017.

[17] G. Wang, F. Gao, R. Fan, and C. Tellambura, "Ambient backscatter communication systems: detection and performance analysis," *IEEE Transactions on Communications*, vol. 64, no. 11, pp. 4836–4846, 2016.

[18] W. Zhao, G. Wang, R. Fan, L.-S. Fan, and S. Atapattu, "Ambient backscatter communication systems: capacity and outage performance analysis," *IEEE Access*, vol. 6, pp. 22695–22704, 2018.

[19] X. Zhou, G. Wang, Y. Wang, and J. Cheng, "An approximate BER analysis for ambient backscatter communication systems with tag selection," *IEEE Access*, vol. 5, pp. 22552–22558, 2017.

[20] H. Guo, Q. Zhang, S. Xiao, and Y.-C. Liang, "Exploiting multiple antennas for cognitive ambient backscatter communication," *IEEE Internet of Things Journal*, vol. 6, no. 1, pp. 765–775, 2019.

[21] R. Long, G. Yang, Y. Pei, and R. Zhang, "Transmit beamforming for cooperative ambient backscatter communication

systems," in *Proceedings of the IEEE Global Communications Conference (Globecom)*, Singapore, December 2017.

[22] G. Yang, Q. Zhang, and Y. C. Liang, "Cooperative ambient backscatter communications for green internet-of-things," *IEEE Internet of Things Journal*, vol. 5, no. 2, pp. 1116–1130, 2018.

[23] G. Yang, Y. C. Liang, and Q. Zhang, "Cooperative receiver for ambient backscatter communications with multiple antennas," in *Proceedings of the IEEE International Conference on Communications (ICC)*, Paris, France, May 2017.

[24] K. H. Jang, S. M. Kim, and J. Kim, "Performance analysis of multi-tag multi-reader ambient backscatter communication systems," in *Proceedings of the IEEE International Conference on Ubiquitous and Future Networks (ICUFN)*, Zagreb, Croatia, July 2019.

[25] D. Mishra and E. G. Larsson, "Multi-tag backscattering to MIMO reader: channel estimation and throughput fairness," *IEEE Transactions on Wireless Communications*, vol. 18, no. 12, pp. 5584–5599, 2019.

[26] Y. Zhang, F. Gao, L. Fan, X. Lei, and G. K. Karagiannidis, "Secure communications for multi-tag backscatter systems," *IEEE Wireless Communications Letters*, vol. 8, no. 4, pp. 1146–1149, 2019.

[27] Y. Liu, Y. Ye, and R. Q. Hu, "Secrecy outage probability in backscatter communication systems with tag selection," *IEEE Communications Letters*, vol. 10, no. 10, 2021.

[28] Y. Jia, W. Gongpu, and Z. Zhangdui, "Physical layer security enhancing transmission protocol against eavesdropping for ambient backscatter communication system," in *Proceedings of the IET International Conference on Wireless, Mobile, and Multimedia Networks (ICWMMN)*, Beijing, China, April 2015.

[29] J. Y. Han, J. Kim, and S. M. Kim, "Physical layer security improvement using artificial noise-aided tag scheduling in ambient backscatter communication systems," in *Proceedings of the IEEE International Conference on Ubiquitous and Future Networks (ICUFN)*, Zagreb, Croatia, July 2019.

[30] J. Y. Han, M. J. Kim, J. Kim, and S. M. Kim, "Physical layer security in multi-tag ambient backscatter communications—jamming vs. coooperation," in *Proceedings of the IEEE Wireless Communications and Networking Conference (WCNC)*, Seoul, South Korea, May 2020.

[31] J. Mitola and G. Q. Maguire, "Cognitive radio: making software radios more personal," *IEEE Personal Communications*, vol. 6, no. 4, pp. 13–18, 1999.

[32] S. Haykin, "Cognitive radio: brain-empowered wireless communications," *IEEE Journal on Selected Areas in Communications*, vol. 23, no. 2, pp. 201–220, 2005.

[33] A. Ahmad, S. Ahmad, M. H. Rehmani, and N. U. Hassan, "A survey on radio resource allocation in cognitive radio sensor networks," *IEEE Communications Surveys & Tutorials*, vol. 17, no. 2, pp. 888–917, 2015.

[34] A. De Domenico, E. Calvanese Strinati, and M.-G. Di Benedetto, "A survey on MAC strategies for cognitive radio networks," *IEEE Communications Surveys & Tutorials*, vol. 14, no. 1, pp. 21–44, 2012.

[35] S. Jha, M. Rashid, V. Bhargava, and C. Despins, "Medium access control in distributed cognitive radio networks," *IEEE Wireless Communications*, vol. 18, no. 4, pp. 41–51, 2011.

[36] L. T. Tan and L. B. Le, "Distributed MAC protocol for cognitive radio networks: design, analysis, and optimization," *IEEE Transactions on Vehicular Technology*, vol. 60, no. 8, pp. 3990–4003, 2011.

[37] S. M. Kim and J. Kim, "Adaptive sensing period based distributed medium access control for cognitive radio networks," *IEICE—Transactions on Communications*, vol. E97-B, no. 11, pp. 2502–2511, 2014.

[38] N. Gul, M. S. Khan, J. Kim, and S. M. Kim, "Robust spectrum sensing via double-sided neighbor distance based on genetic algorithm in cognitive radio networks," *"Mobile Information Systems*, vol. 2020, Article ID 8876824, 10 pages, 2020.

[39] M. S. Khan, J. Kim, E. H. Lee, and S. M. Kim, "An efficient contention-window based reporting for Internet of things features in cognitive radio networks," *Wireless Communications and Mobile Computing*, vol. 20199 pages, 2019.

[40] D. T. Hoang, D. Niyato, P. Wang, D. I. Kim, and Z. Han, "Ambient backscatter: a new approach to improve network performance for RF-powered cognitive radio networks," *IEEE Transactions on Communications*, vol. 65, no. 9, pp. 3659–3674, 2017.

[41] H. Guo, Q. Zhang, S. Xiao, and Y.-C. Liang, "Multi-antenna beamforming receiver for cognitive ambient backscatter communications," in *Proceedings of the IEEE Global Communications Conference (Globecom)*, Abu Dhabi, United Arab Emirates, December 2018.

[42] H. Guo, R. Long, and Y.-C. Liang, "Cognitive backscatter network: a spectrum sharing paradigm for passive IoT," *IEEE Wireless Communications Letters*, vol. 8, no. 5, 2019.

[43] T. Taesang Yoo and A. Goldsmith, "Capacity and power allocation for fading MIMO channels with channel estimation error," *IEEE Transactions on Information Theory*, vol. 52, no. 5, pp. 2203–2214, 2006.

[44] X. Kang, H. F. Chong, Y.-K. Chia, and S. Sun, "Ergodic sum-rate maximization for fading cognitive multiple-access channels without successive interference cancelation," *IEEE Transactions on Vehicular Technology*, vol. 64, no. 9, pp. 4009–4018, 2015.